The Critical Transition Length from Chapman-Jouguet Deflagrations to Detonations

Mohamed Saif[1], A. Pekalski[2], M. Levin[3] and M.I. Radulescu[1]+

[1]*Department of Mechanical Engineering, University of Ottawa, Canada K1N 6N5*
[2]*Shell Global Solutions (UK)*
[3]*Shell Exploration & Production Company (SEPCO)*

+ Presenter E-mail: matei@uottawa.ca

Abstract

In the process of deflagration-to-detonation transition (DDT) in reactive gases, the flame typically accelerates first to the choked flame condition (known as a Chapman-Jouguet deflagration), where it propagates at the sound speed with respect to the product gases. Subsequently, the choked flame may transit to a detonation. In the present study, the transition length from choked flames to detonations was measured experimentally in laboratory-scale experiments in methane, ethane, ethylene, acetylene, and propane with oxygen as oxidizer. The choked flames were first generated following the quenching of an incident detonation after its interaction with cylindrical obstacles. The subsequent acceleration was monitored via large-scale time-resolved shadowgraphy. The mechanism of transition was found to be through the amplification of transverse waves and hot spot ignition from local Mach reflections. The transition length was found to correlate very well with the mixture's sensitivity to temperature fluctuations, reflected by the □ parameter introduced by Radulescu, which is the product of the non-dimensional activation energy (E_a/RT) and the ratio of chemical induction to reaction time (t_{ig}/t_r). Mixtures with a higher □ parameter were found more susceptible to hot spot ignition and had a transition length much shorter than anticipated from a model neglecting the fluctuations in the choked flame structure. The correlation between transition length and the □ parameter ob[...] oxygen sub-atmospheric experiments was used to determine the critical DDT lengths in the same fuels with air as oxidizer at ambient pressures, thus providing an estimate for the critical charge dimension of reactive gases necessary to initiate a detonation.

Introduction

The accidental release of a flammable mixture (for example, in a processing plant or during transport) may lead to the formation of a flammable gas cloud. If the flammable cloud ignites, an explosion can occur, especially if the cloud envelops a congested area. When a reactive cloud is

ignited, an initially low speed subsonic flame accelerates owing to various instability mechanisms and possible interactions with confining structures and obstacles [1, 2]. The early stages of this subsonic flame acceleration are relatively well understood and modeled. The acceleration of this subsonic flame culminates with the establishment of a wave propagating close to the sound speed in the burned products with respect to them, called a choked flame [3]. The subsequent transition of this choked flame into a detonation is much less understood. Such extreme events can lead to substantial over-pressures (in excess of a few atmospheres), which may cause severe losses.

Flame acceleration and transition to detonation in industrial scale accidents was recently reviewed by Pekalski et al. [4], who have also performed large scale tests in ethane-air mixtures and demonstrated that flames may accelerate to detonations in unconfined and partly congested areas. There are also previous accidents where detonations are believed to had happened [4]. The Buncefield incident in the UK (2005) [5] has shown that DDT can occur in actual commercial-scale facilities, producing a devastating effect, an interruption of business, and a significant impact on company/industry reputation. DDT also occurred in the Jaipur incident in India [6], leading to 11 fatalities.

The transition length from choked flames to detonations was proposed as a measure for the detonation propensity, as it controls whether a given reactive mixture will transit to a detonation in a particular geometry, as related to the characteristic free-path in a congested area [7]. The transition from fast deflagration to detonation is also believed to be universal in all types of detonation initiation. The DDT length can thus provide a useful measure of critical reactive cloud dimension of sufficient extent to sustain a detonation. Previous work has suggested that this critical transition length can be correlated with the detonation cell size [7], yielding to the called 7 $\square$ criterion. Nevertheless, cell sizes are very difficult to measure and only available in limited reacting mixtures and operating conditions [8]. There is currently a need to predict or relate this critical length scale to the thermo-chemical properties of the mixture.

In the present study, we measure the DDT length in laboratory scale experiments in different hydrocarbon-oxygen mixtures and correlate it to the relevant thermo-kinetic parameters of the mixtures. The correlation for the DDT length is then extended to fuel-air mixtures at ambient conditions. We focus on the acceleration of fast deflagrations, recently shown to be well approximated as Chapman-Jouguet deflagrations [9].

Recent experiments performed in methane-oxygen mixtures by Maley et al. [10] revealed the propagation mechanism of the choked flames. The authors isolated these flames by allowing a CJ detonation wave to quench after interacting with a set of obstacles. The subsequent shock flame structure propagated by punctuated hot spot ignitions. The same set-up was also used by Chao [11] and by Grondin and Lee [12], who noted differences between mixtures characterized with weakly or strongly dependent reaction rates temperature fluctuations.

Recently, Radulescu et al. [13] proposed a non-dimensional parameter to characterize the detonability of reactive mixtures, namely,

$$\chi = \frac{E_a}{RT}\frac{t_{ig}}{t_r}$$

where (E_a/RT) is the reduced activation energy, (t_{ig}) is the ignition delay time and (t_r) is the reaction time. This parameter has also been suggested to control the propensity for hot spot formation in the presence of temperature fluctuations, detonation stability, the propensity for engine knock, and the local acceleration of one-dimensional fast flames to detonations. The present study examines whether a correlation can be drawn between the DDT length in various mixtures and this parameter.

Experimental Details

The experiments were conducted in a 3.4-m-long thin rectangular channel, 203-mm-tall and 19-mm wide, as described by Maley et al. [10] and shown schematically in Figure 1. The last meter of the channel was equipped with glass windows allowing the visualization of the flow evolution via high-speed large scale shadowgraphy. The imaging used 42,049 frames per second (interframe time of 23.8 μsec) and 1152 by 256-pixel resolution, corresponding to a spatial resolution of approximately 1 mm.
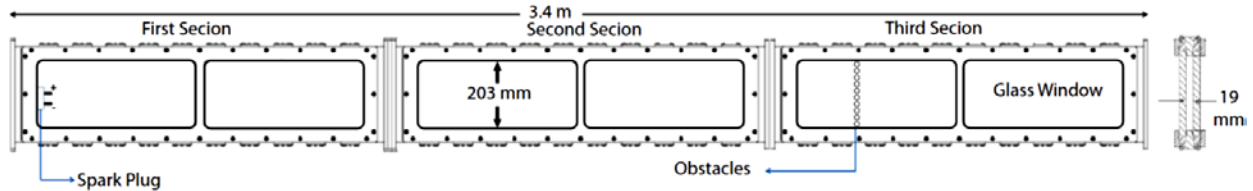

Figure 1: Schematic of shock tube apparatus with ten obstacles.

A row of cylindrical obstacles of 16-mm-diameter were placed at the entrance of the visual section of the shock tube to allow for visualization of the fast flames established downstream. This corresponded to a area blockage ratio of the obstacles of 75%. Fig. 2 shows the test section.

The mixtures studied were stoichiometric methane, propane, ethane, ethylene, and acetylene with oxygen. The acetylene mixture was diluted with 75% argon per mole, and offered a mixture with a much lower propensity for hot spot formation, as indicated by its low value of χ, as described below. The gasses were mixed in a separate vessel and left to mix for a minimum of 24 hours before an experiment. Varying the initial pressure, p_0, of the test mixture permitted us to control the reactivity of the mixture.

Results

<u>Methane</u>

Figure 2 shows a multi-frame overlay of a typical test, here in stoichiometric methane-oxygen at 8.2 kPa initial pressure. The wave front is propagating from left to right. Frame 1 shows a propagating CJ detonation wave. Frame 2 shows the interaction with the obstacles. A complex of shock waves are reflected from the obstacles and transmitted across. The transmitted shocks are

driven by the jets exiting between the obstacles. Frame 3 shows distinct re-ignition regions be-hind the lead shock, as described by Maley et al.[10]. Shortly after, in Frame 4, the lead shock front organizes into a very corrugated shock-flame complex. In Frames 5, 6 and 7, the front re-organizes with only two Mach reflections. The structure resembles quite closely the structure of unstable cellular detonations [14], but propagates at an average speed approximately 30% lower than the CJ speed, as shown in Fig. 3. For reference, Fig. 3 also shows two speed predictions for the lead shock, the first assuming assuming the flame is a CJ deflagration, while the second as-suming the burning speed is negligibly slow and does not affect the motion of the transmitted shock [9].
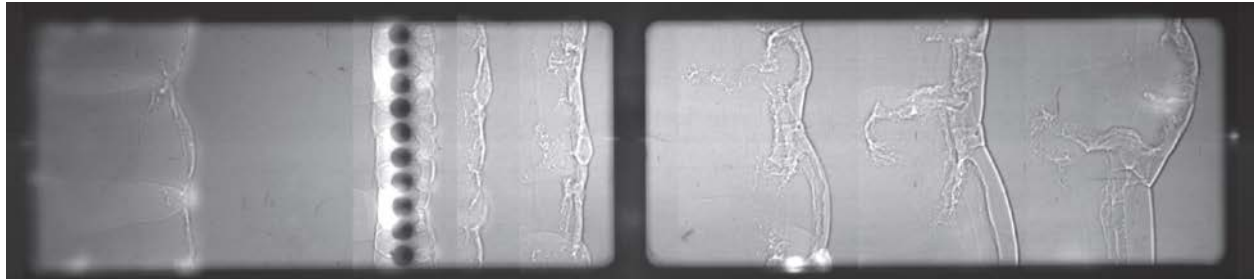

Figure 2: Overlay of multiple shadowgraph video frames showing the evolution of the wave front in a methane-oxygen mixture at $p_0 = 8.2$ kPa (1.2 psi); wave propagates from left to right.
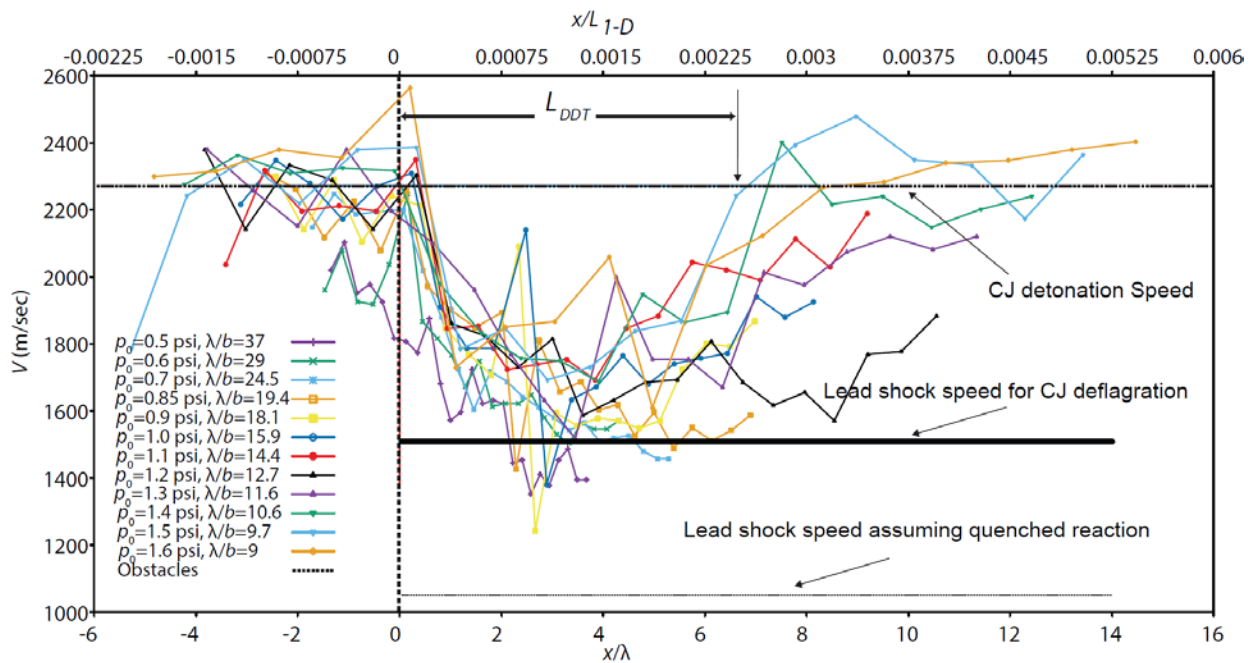

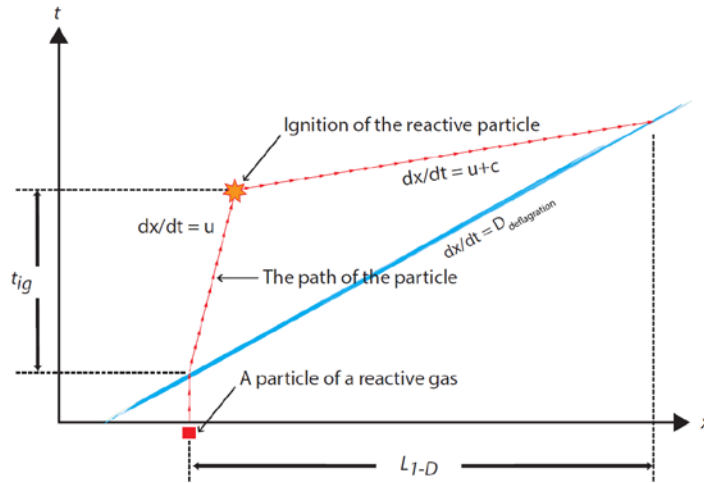Figure 3: Lead shock speed for the methane-oxygen tests.

Figure 4: A space time diagram illustrating the L_{1-D} distance.

Figure 3 shows the lead shock speeds recorded for all the tests performed in methane-oxygen mixtures. For each test, the position of the lead shock was registered at five equally spaced locations along the shock, then averaged in order to obtain the mean position of the shock. The average speed reported is thus an average value. After the interaction with the obstacles, the shock-flame complex propagates at approximately 65% of the CJ detonation speed (1490-1510 m/s), in good agreement with the CJ deflagration speed calculated by Radulescu et al. [9]. The fast flames subsequently accelerate to a detonation. It is interesting to notice that even for lower pressure cases, the flame-shock systems maintained their speed above/equal to the theoretical CJ deflagration speed.

The distance traveled by the fast flames from the obstacles to where they reach DDT is labeled L_{DDT} in Fig. 3. When normalized by the detonation cell size λ, obtained from Shepherd's detonation database [8], the DDT length L_{DDT}/λ is 7 over the entire range of pressures (p_0) ranging between 0.5 psi to 1.6 psi. This is in excellent agreement with the correlation recommended by Dorofeev for the critical DDT length [7].

We also compared the DDT length with a characteristic length L_{1-D} that a 1D shock, traveling at the computed CJ deflagration speed, would travel before transiting to a detonation. The definition of this length scale is shown in Figure. 4. This distance is the distance traveled by the lead shock such that the feedback from a particle of gas ignited by the shock is felt by the shock at a later time. Consider a particle of gas being shocked. The particle is convected at speed u and ignites after a time (t_{ig}). After ignition, a forward facing compression wave propagating at speed $u+c$ catches up to the shock. The state behind the shocks was computed using the NASA CEA code, while the ignition delays were evaluated assuming negligible specific volume change using CANTERA and the GRI-3.0 mechanism.

The DDT length measured, when normalized by L_{1-D}, was found to also be relatively invariant for all the tests performed, yielding approximately $L_{DDT}/L_{1-D} \sim 0.003$. That this ratio is significantly less than unity clearly highlights the important role played by local hotspots, shortening the DDT length.

Propane

The shock speed histories obtained for the propane mixtures are shown in Figure 5, for pressures ranging between 0.3 psi to 0.8 psi. When correlated with the detonation cell size, the transition length was found in good agreement with Dorofeev's 7 L_{DDT}/λ ratio of approximately-yielding proximately 8. When normalized by the theoretical DDT length, L_{DDT}/L_{1-D} was approximately 0.01, larger than for the methane tests. The calculations for propane were performed with the Sandiego mechanism. For the tests conducted at 0.55, 0.6, 0.7, 0.8 psi, velocities for the shock flame complex before the transition were found to be in the range of 1400 to 1600 m/s, approximately 65% of CJ detonation and equal to the calculated CJ deflagration speed. After 4λ, they start to accelerate until they reach CJ detonation. For tests conducted at 0.3, 0.4, 0.5 psi, the wave front speeds dropped to lower velocities between the CJ deflagration and inert shock speeds (1000 -1400 m/s).

Figure 6 shows the same pattern as methane from frame 1 to 4, but one of the shock-shock reflections initiated a detonation wave that engulfed the original one, as seen in frames 5, 6 and 7.
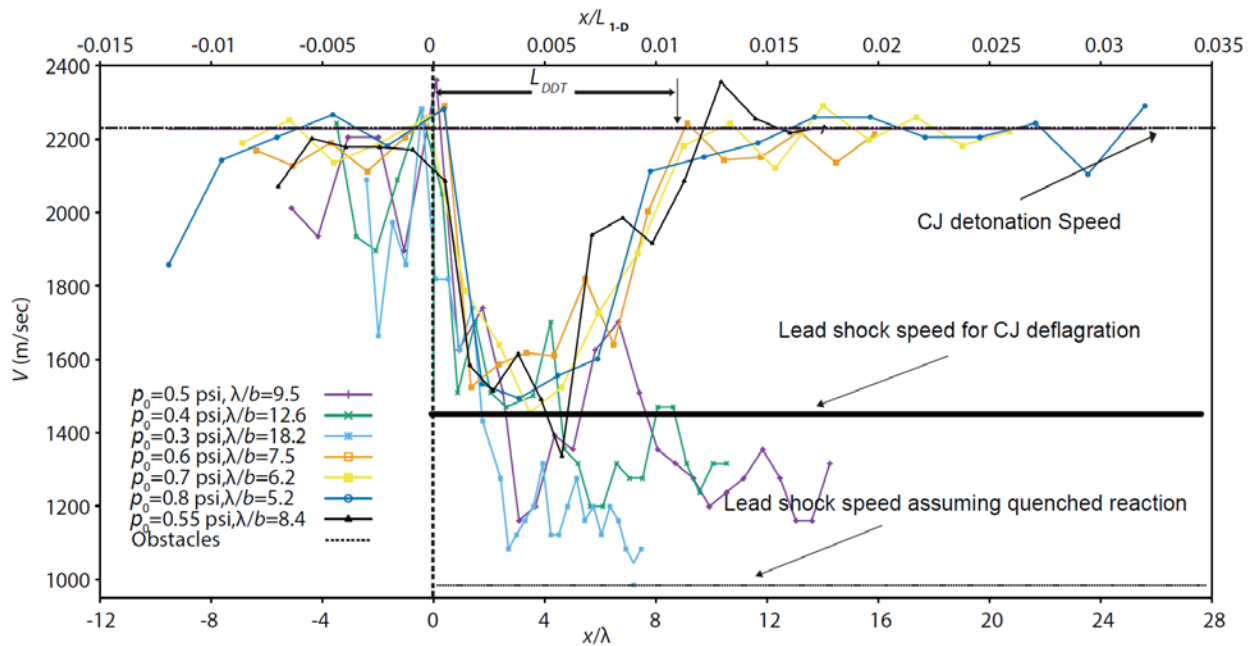

Figure 5: Lead shock speed for the tests conducted in propane-oxygen mixtures.
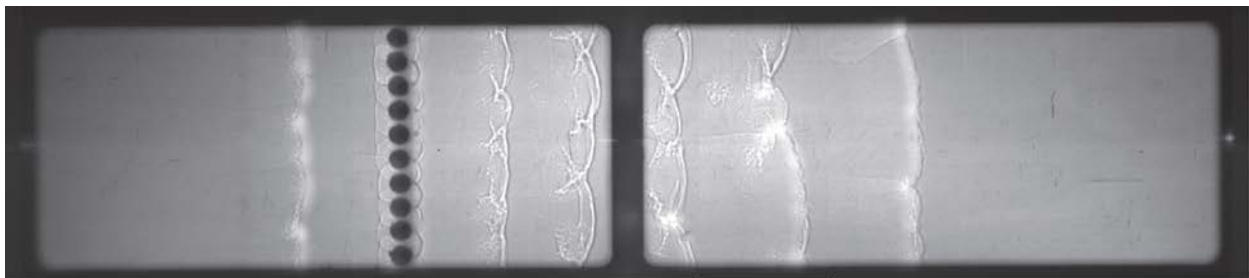

Figure 6: Overlay of multiple shadowgraph video frames showing the evolution of the wave front in a propane-oxygen mixture at $p_0 = 3.8$ kPa (0.55 psi).

Ethane

Figure 7 shows the results of the tests conducted for ethane at initial pressures p_0 ranging between 0.3 psi and 0.8 psi. After interactions, all velocities dropped close to the computed CJ deflagration speed (1440-1450 m/s) and continued for a distance about two cells size. For tests conducted between 0.35-0.45 psi, they continued to drop, to speeds corresponding to a negligible infunece of energy release (1011 m/s). As for tests at 0.5 psi and above, they all accelerated rapidly to CJ detonations. Critical values for L_{DDT}/L_{1-D} were in the range of 0.005-0.01. The calculations were performed with the Sandiego mechanism. L_{DDT}/λ was approximately 5-10.
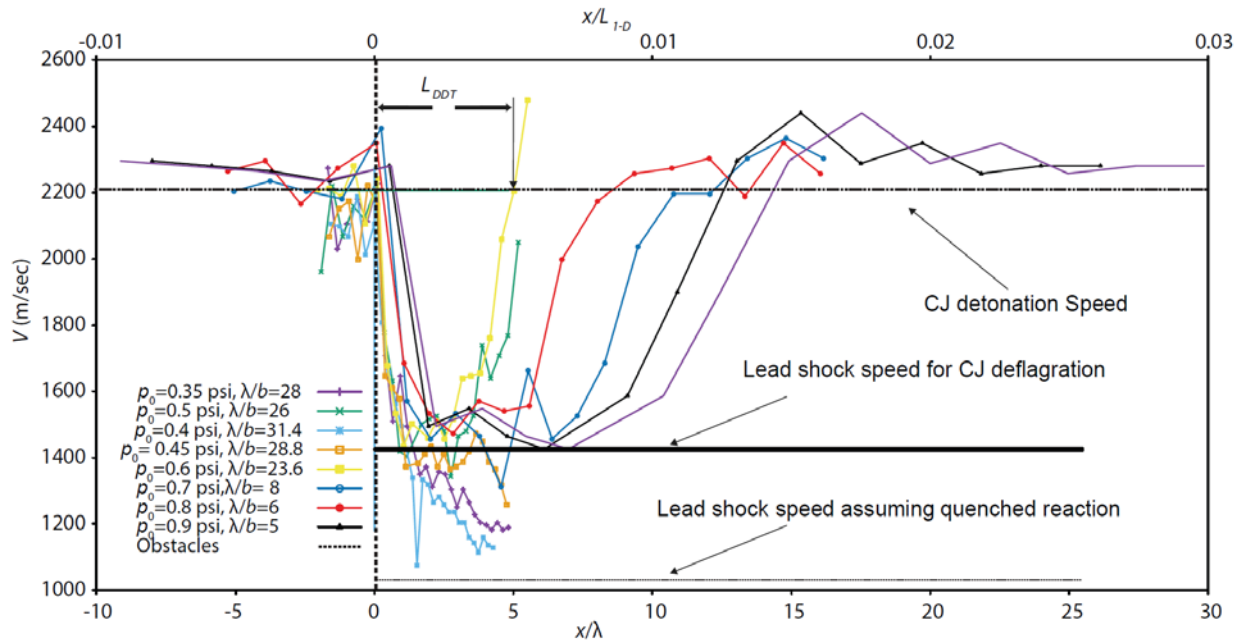

Figure 7: Lead shock speed for the tests conducted in ethane-oxygen mixtures.

Figure 8: Overlay of multiple shadowgraph video frames showing the evolution of the wave front in an ethane-oxygen mixture at $p_0 = 3.4$ kPa (0.5 psi).

Figure 8 shows an example of the lead front dynamics in an ethane mixture. The choked flame amplification dynamics are qualitatively similar to propane and methane with the organization of the front into fewer stronger modes before the final detonation initiation in the last two frames.

Ethylene

Figure 9 shows the results obtained for ethylene-oxygen mixtures. L_{DDT}/L_{1-D} for ethylene was 0.03-0.07, and L_{DDT}/λ was 15-30. The calculations were performed with the Sandiego mechanism. For all tests between (p_0) 0.5 - 1.0 psi, the velocities dropped close to CJ deflagration (1480-1490 m/s). The velocity at test 0.5 psi decayed further and the front propagated around 1200 m/s. All the remaining tests for higher pressures accelerated after a distance equal to 5 λ and reached CJ detonation. Figure 10 shows an example of DDT, yielding a similar sequence to the other mixtures described above.
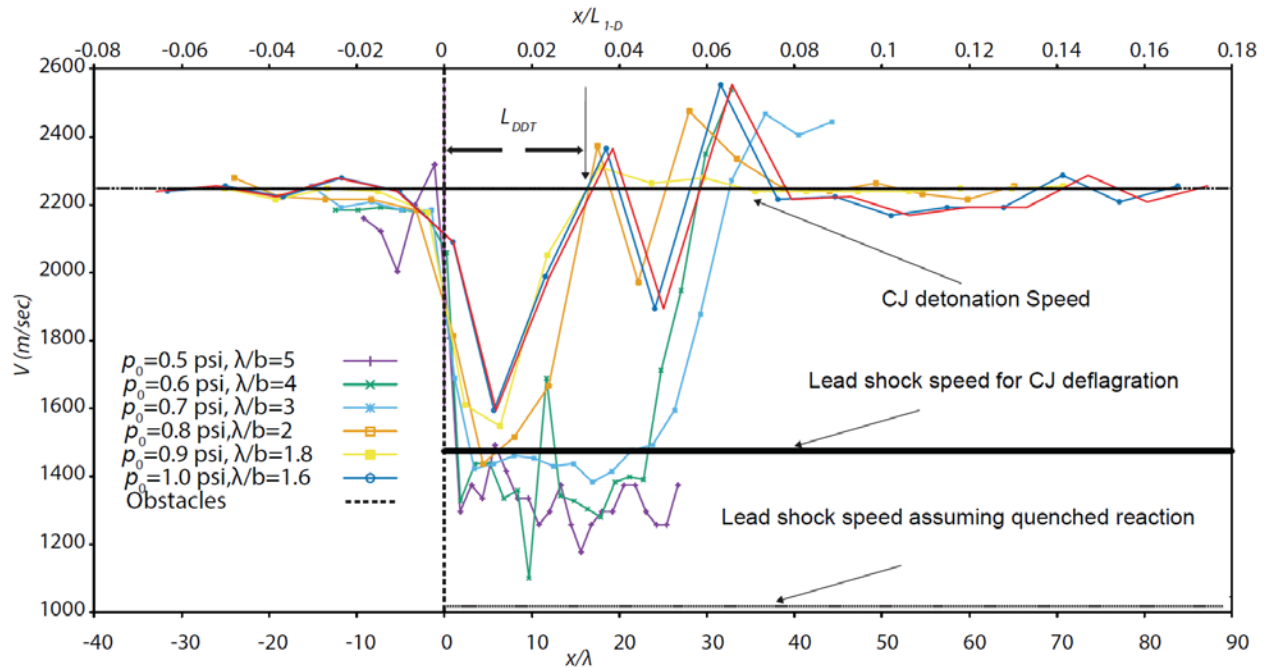

Figure 9: Lead shock speed for the tests conducted in ethylene-oxygen mixture.
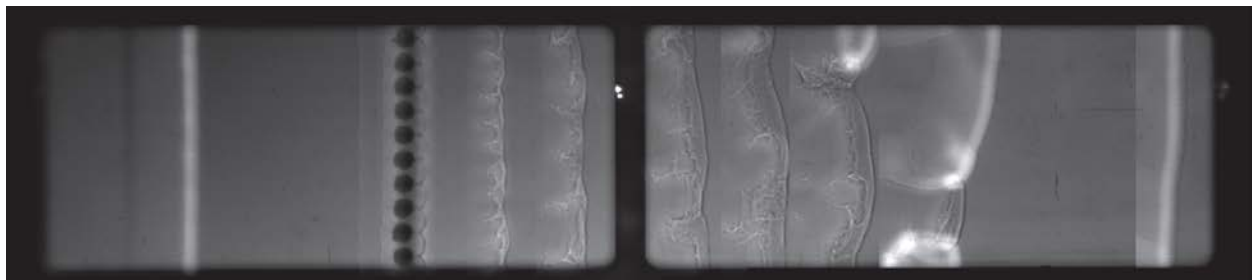

Figure 10: Overlay of multiple shadowgraph video frames showing the evolution of the wave front in an ethylene-oxygen mixture at $p_0 = 4.8$ kPa (0.7 psi).

Acetylene with argon dilution

Figure 11 shows the results for the tests conducted in acetylene for initial pressures p_0 ranging between 1.4 psi and 1.6 psi. The critical L_{DDT}/L_{1-D} was 0.8, and L_{DDT}/λ was 20. The calculations were performed with the Sandiego mechanism. For all the tests conducted, after the interaction they dropped to deflagration speeds of 1300m/s and kept propagating for only 3 or 5 λ distance. They transit almost immediately into CJ detonation speed, except for the test conducted at

1.4 psi, where the speeds dropped dramatically to 800m/s, which was close to the prediction made assuming the lead shock is not supported by the flame energy release.

Figure 12 and 13 shows that acetylene adopted the same sequence of events as the previous mixtures, up to the point where they formed the keystone structures at frame 3. In figure 13, the shock front decoupled from the flame front, and the gap between them kept increasing until the end of the channel, as for figure 12, detonation was initiated from the reflections generated after the obstacles. For all cases, there was no corrugated flame-shock complex generated, as in methane or propane cases.
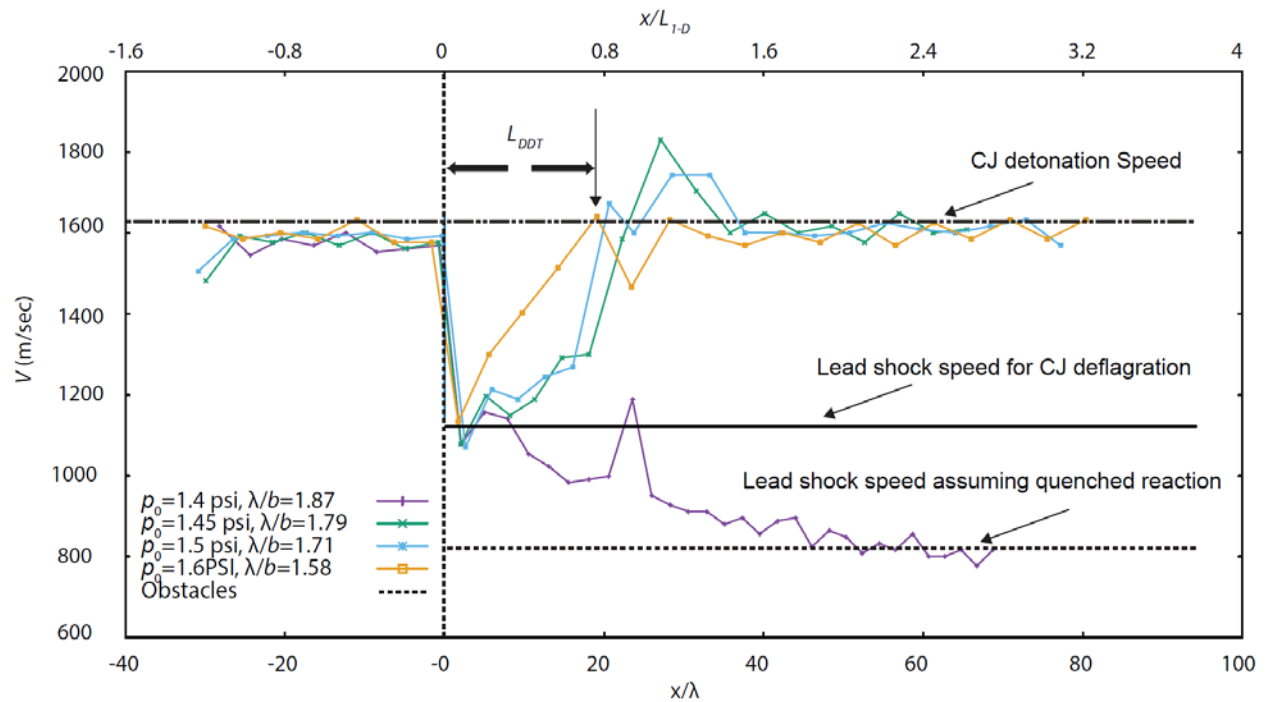

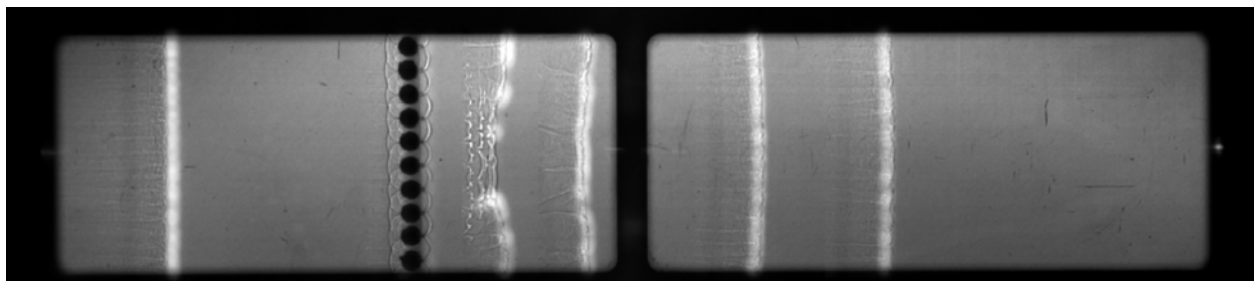Figure 11: Lead shock speed for the tests conducted in acetylene-oxygen-argon mixture

Figure 12: Overlay of multiple shadowgraph video frames showing the evolution of the wave front in an acetylene-oxygen-argon mixture at $p_0 = 11$ kPa (1.6 psi).

Figure 13: Overlay of multiple shadowgraph video frames showing the evolution of the wave front in an acetylene-oxygen-argon mixture at p_0 = 9.6 kPa (1.4 psi).

Summary and conclusion

The measured DDT length for all the mixtures studied was found to correlate relatively well with Dorofeev's 7 ⬜rcfhemorthane, ethane and propane tests. Some departures were observed however for ethane, ethylene and acetylene, by factors of 3-4. This suggests that such a correlation can provide a useful order of magnitude estimate for the critical DDT conditions.

Figure 14 shows the variation of L_{DDT}/L_{1-D} with the hotspot parameter χ. A clear correlation is apparent for the tests performed in the different mixtures. The higher the value of χ, the shorter the run-up distance when normalized by L_{1-D}. This supports the view that the acceleration of the choked flames is enhanced in mixtures where hot spots are more readily developed, as discussed by Radulescu et al. [13].
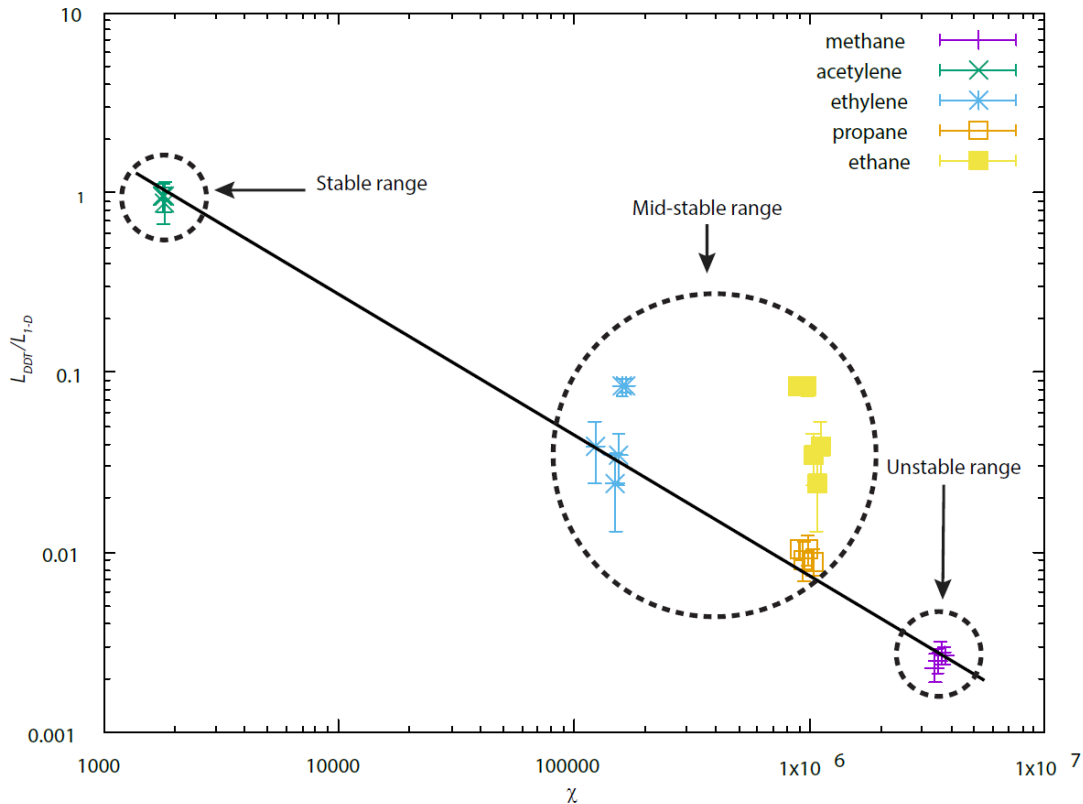

Figure 14: Variation of the normalized DDT transition length L_{DDT}/L_{1-D} with the hot spot parameter χ for methane, propane, ethane, ethylene, and acetylene.

Looking back at the velocity plots, we observed that the lead velocity of methane did not fall below the calculated CJ deflagration speed. That was the case for all the tests conducted, even at lower initial pressures. Propane, ethane, and ethylene adopted the same pattern for high and mid initial pressures. However, for lower pressure cases, the front shock decoupled from the flame

Mixture	χ	$L_{\text{1-D}}$ (m)	L_{DDT} (m)
CH_4-Air	1.3×10^7	2584.5	5.7
C_2H_2-Air	9.2×10^5	55.8	0.78
C_3H_8-Air	7.5×10^5	66.6	1.08
C_2H_4-Air	2.4×10^5	18.05	0.65
C_2H_6-Air	1.2×10^6	109	1.28

and the gap between them kept increasing to the end of the channel. The acetylene tests were quite different, they adopted the go-no go behavior for the entire tests conducted, and that depended directly on the sensitivity of the fuel (the initial pressure of the mixture).

Using the trend line from Figure 14, a correlation of the DDT length takes the form:

$$\frac{L_{DDT}}{L_{1-D}} = 193.93 \, \chi^{-0.694}$$

Using this correlation, the run-up-distance to detonation (L_{DDT}) can be estimated for different mixtures and operating conditions, provided L1D can be evaluated using the available termo and chemical data. Here, we considered all the previous mixtures, but using air as an oxidizer, and 1 atm as initial pressure. The results are shown in Table 1. All the mixtures considered yield critical distances on the order of 1 meter, while methane is found the least sensitive, requiring a critical amplification length of approximately 6 m.

Table 1: Calculated values of χ, L_{1D} and L_{DDT} for fuel-air mixtures at ambient conditions.

Acknowledgements

References

1.   Lee, J.H.S., Moen, I.O., *The mechanism of transition from deflagration to detonation in vapor cloud explosions*. Progress in Energy and Combustion Science 1980; **6**: p.359-89.
2.   Ciccarelli. G., Dorofeev, S., *Flame acceleration and transition to detonation in ducts*. Progress in Energy and Combustion Science 2008; **34**: p.499-550.
3.   Lee, J.H.S. *The detonation phenomenon*. Cambridge; New York: Cambridge University Press; 2008.
4.   Pekalski, A., Puttock, J., Chynoweth, S., *DDT in a vapour cloud explosion in unconfined and congested space: large scale test*. Tenth International Symposium on Hazards, Prevention, and Mitigation of Industrial Explosions. Bergen, Norway, 2014.

5.   Newton, A.H., *The Buncefield incident: 11 December 2005*. The final report of the Major Incident Investigation Board. London, UK, 2008.

6.   Johnson, D.M., *Vapour cloud explosion at the IOC terminal in Jaipur*. Hazards XXIII, Symposium Series, No. 158, IChemE, 2012: p.556-64.

7.   Dorofeev, S.B., Sidorov, V.P., Kuznetsov, M.S., Matsukov, I.D., Alekseev, V.I. *Effect of scale on the onset of detonations*. Shock Waves 2000; **10**: p.137-49.

8.   Kaneshige, M., Shepherd, J.E., *Detonation Database*, Technical Report FM97-8, GALCIT, July 1997. See also the electronic hypertext version at
 http://www.galcit.caltech.edu/detn_db/html/.

9.   Radulescu, M.I., Wang, W., Saif, M., Maley, M., Levin, M., Pekalski, A., *On Chapman Jouguet deflagrations*. In: Radulescu MI, ed. 25th International Colloquium on the Dynamics of Explosions and Reactive Systems. Leeds, UK, 2015.

10.   Maley, L., Bhattacharjee, R., Lau-Chapdelaine, S.M., Radulescu, M.I. *Influence of hydrodynamic instabilities on the propagation mechanism of fast flames*. Proceedings of the Combustion Institute 2015; **35**: p.2117-26.

11.   Chao, J.C., *Critical deflagration waves that lead to the onset of detonation*. 2006 Ph.D. Thesis, McGill University, Montreal, Canada.

12.   Grondin, J.S., Lee, J.H.S., *Experimental observation of the onset of detonation downstream of a perforated plate*. Shock Waves 2010; **20**: p.381-6.

13.   Radulescu, M.I., Sharpe, G.J., Bradley, D., *A universal parameter quantifying explosion hazards, detonability and hot spot formation, the* χ *number*. In: Bradley D, Makhviladze G, Molkov V, Sunderland P, Tamanini F, eds. Seventh International Seminar on Fire & Explosion Hazards. Providence, Rhode Island: Research Publishing University of Maryland, 2013.

14.   Radulescu, M.I., Sharpe, G.J., Law, C.K., Lee, J.H.S. *The hydrodynamic structure of unstable cellular detonations*. Journal of Fluid Mechanics 2007; **580**: p.31-81.